INTERNATIONAL JOURNAL FOR NUMERICAL METHODS IN FLUIDS, VOL. 18, 1107–1119 (1994)

TRANSPORT OF RADIONUCLIDES IN ISOLATED FRACTURES IN CRYSTALLINE ROCKS

G. M. GRANDI AND J. C. FERRERI*

CNEA, Gerencia de Seguridad Radiológica y Nuclear Av. Libertador 8250, 1429 Buenos Aires, Argentina

SUMMARY

This paper presents a generalization of a computational method for the prediction of solute dispersion in fractured porous media. This method is specially useful for the prediction of subsurface flows in crystalline rocks. The model now includes a linear kinetics mechanism to represent the effects of sorption of radionuclides in the rock matrix. The method is improved in its accuracy and provides results useful for the assessment of radionuclide migration in high-level, radioactive waste repositories. Results including verification (analytical) and physical test simulations are given. These results provide a partial validation of the numerical model.

KEY WORDS Fractured porous media Radionuclide migration Repositories modelling Boundary fitted Finite difference method

INTRODUCTION

The accurate prediction of the hydrodynamics of fractured porous media and the dispersion of contaminants in such media is of primary importance in many applications. The present paper deals with a particular case, namely the assessment of the impact of high-level, radioactive waste repositories. The physical and numerical aspects of this type of simulation have been considered previously.[1–6] Reference 6 gives details of a numerical method to predict subsurface flows in crystalline, fractured rocks under the influence of geophysical and thermal gradients. A simple instantaneous equilibrium model was used in Reference 6 to consider the dispersion of passive contaminants. This model worked very well in several cases of interest dealing with dispersion from isolated fractures. However, it was soon realized that the limitations implied in the model could degrade the results in more general situations. It was thus decided to improve both the physical model and the numerical representation of the interface dynamics of contaminant concentration.

The conceptual model consists of an equivalent porous medium and discrete fractures, in the sense defined previously by the authors.[6] In this way a combination of the properties of continuum models and the advantages of considering fully discrete models for macroscopic fractures is obtained. It is important to recall here that the latter are the ones dictating the flow pattern, giving the appropriate interface between the macroscopic flow and the local rock conditions responsible for contaminant sorption. Then the properties in the bulk medium are obtained by averages, including the microfactures in volumes of apporpriate size. Strong anisotropies are considered through macroscopic fractures. The model considers integral mass

* Member of CONICET, Argentina.

CCC 0271–2091/94/111107–13

Received 8 December 1992
Revised 19 November 1993

formulations that avoid source terms and internal boundary conditions between the factures and the porous medium.

In the following sections the governing equations in the physical domain are introduced. Only a brief mention of the numerical technique is made. Finally, results corresponding to the numerical simulation of an analytical solution and a tracer experiment are shown.

THEORETICAL MODEL

The theoretical model will be established considering the equivalent porous medium and the discrete fractures separately.

The following hypotheses[5,7] are considered for the equivalent porous medium.

1. It is saturated.
2. The solute (a radionuclide) is inert. This means that it does not affect the solvent (water) physical properties. However, it interacts with the rock matrix through its surface ('sorption').
3. The rock matrix is non-deformable.

The transport mechanisms considered are[5]

(a) advection due to water flow
(b) molecular diffusion in the water
(c) mechanical dispersion due to velocity and concentration in the rock pores (the effects of molecular diffusion and mechanical dispersion are grouped as 'hydrodynamic dispersion')
(d) adsorption in the porous matrix
(e) radioactive decay for the solute.

The equation describing solute advection–diffusion in the equivalent porous medium may be written as[6]

$$\left(\phi \frac{\partial C}{\partial t} + \bar{q}\nabla C - \nabla\phi D\nabla C + \phi\lambda C\right) + (1-\phi)\rho_B\left(\frac{\partial F}{\partial t} + \lambda F\right) = 0. \tag{1}$$

The meanings of the different variables are given in the Appendix.

Under typical respository flow conditions in a crystalline rock (low velocities and long residence times), equilibrium between the adsorbed solute concentration (F) and the solute concentration in the fluid (C) may usually be assumed. However, a linear kinetics equation will be considered to relate the two quantities. This will prove to be useful in what follows

Thus

$$\left(\frac{\partial F}{\partial t} + \lambda F\right) = K_S^P C - K_R^P F. \tag{2}$$

If equilibrium conditions prevail—the mixing is instantaneous—and additionally the radionuclide is table ($\lambda = 0$), equation (2) reduces to

$$F = \frac{K_S^P}{K_R^P} C = K_D C. \tag{3}$$

The transport mechanisms considered for discrete fractures are similar to those considered for a microfissured rock. The working hypotheses are as follows.

1. The facture aperture is small compared with its length.

2. Transverse diffusion and longitudinal dispersion in the fracture ensure complete mixing of the solute in the solvent. Thus a one-dimensional approach is applied to model transport effects in the fractures.

The transport mechanisms considered are[5]

(a) one-dimensional advection along the fracture
(b) longitudinal mechanical dispersion and molecular diffusion
(c) diffusion towards/from the porous matrix surrounding the fracture
(d) adsorption at fracture walls
(e) radioactive decay of the solute.

Thus the transport equation for the solute along a discrete fracture is

$$\left(\frac{\partial C}{\partial t} + \bar{u}_f \frac{\partial C}{\partial l} - \frac{\partial}{\partial l} D_L \frac{\partial C}{\partial l} + \lambda C\right) + \frac{1}{b}\left(\frac{\partial S}{\partial t} + \lambda S\right) = \dot{M}, \tag{4}$$

where

$$D_L = \alpha_L |\bar{u}_f| + \beta_L |\bar{u}_f|^2.$$

References 8–12 give a detailed analysis of the influence of dispersion coefficients in the transport equation, together with expressions for their calculation.

A linear kinetics equation is also assumed to relate the solute fluid concentration (C) to the solute concentration per unit area of the fracture/porous medium interface. Thus

$$\left(\frac{\partial S}{\partial t} + \lambda S\right) = bK_S^F C - K_R^F S. \tag{5}$$

Under the same conditions mentioned above for equation (2), equation (4) reduces to

$$F = b \frac{K_S^P}{K_R^P} C = K_A C. \tag{6}$$

RADIONUCLIDE TRANSPORT EQUATION IN AN EQUIVALENT POROUS MEDIUM WITH DISCRETE FRACTURES

The governing equation for the transport of radionuclides (the inert solute) in a control volume results from the combination of equations (1), (2) and (4), (5). It is important to recall that fractures are included in the two-dimensional control volumes as one-dimensional paths. Thus a single value of C represents the concentration of the solute in the porous medium and the fracture (see Reference 6 for details).

Thus the following expression is obtained:

$$\int_{\mathscr{V}-\mathscr{V}_f} \left[\phi\left(\frac{\partial C}{\partial t} + \lambda C\right) + (1-\phi)\rho_B(K_S^P C - K_R^P F)\right] d\mathscr{V} + \int_{\mathscr{V}_f} \left(\frac{\partial C}{\partial t} + \lambda C + K_S^F C - \frac{1}{b} F_R^F S\right) d\mathscr{V}$$
$$+ \int_{\partial(\mathscr{V}-\mathscr{V}_f)_{ext}} [(\bar{q}\cdot\bar{n})C - D\phi\nabla C\cdot\bar{n}]\, d\mathscr{A} + \int_{\partial(\mathscr{V}_f)_{ext}} \left((\bar{u}_f\cdot\bar{n})C - D_L\frac{\partial C}{\partial l}\cdot\bar{n}\right) d\mathscr{A} = 0. \tag{7}$$

In equation (7) the unknowns are C, F and S. Fluid velocities are considered as data, as given by a hydrodynamics code. The code described in Reference 6 was used in our calculations. Rock properties and all the parameters needed to close the system are considered as data.

NUMERICAL METHOD

Equation (7) has been solved using a boundary-fitted finite difference method which allows for adapting the computational grid to the boundaries of the domain. These boundaries may be external (the limits of the integration domain) or internal (a mesh of discrete fractures). The difference equations resulting from the discretization were solved using a fully implicit technique. A detailed version of the algorithms and several applications may be found in Reference 6. Reference 5 gives further details on the technique.

RESULTS

Case 1

The first case considered in the present calculations was obtained from Reference 8. It consists of predicting the transport of a single radionuclide along an isolated horizontal fracture in an otherwise uniform rock. The fracture has constant aperture δ. Water injection from a well of radius r_0 proceeds at constant flow rate Q. The flow is assumed axisymmetric and diverging from the well. Water is assumed to flow along the fracture. The rock is assumed to have low enough hydraulic conductivity to justify this hypothesis. Figure 1 shows the geometry of the problem.

Thus the radionuclide is transported along the fracture and dispersed in the porous rock. Boundary conditions imposed for the numerical simulations are compatible with this scenario.

Problem parameters are as follows: $\delta = 0{\cdot}0001$ m, $Q = 1{\cdot}16 \times 10^{-7}$ m^3 s^{-1}, $\alpha_L = 0{\cdot}5$ m, $\beta_L = 0$ s^{-1}, $\lambda = 1{\cdot}7785$ s^{-1}, $r_0 = 0{\cdot}11$ m, $\rho_B = 2700$ kg m^{-3}, $\phi = 0{\cdot}01$, $D = 1{\cdot}6 \times 10^{-10}$ m^2 s^{-1}.

Case 1(a). For this example it was assumed that adsorption in the rock did not exist. Thus $K_D = 0$ m^3 kg^{-1} and $K_A = 0$ m.

The integration domain was subdivided by a variable computing mesh consisting of 25 nodes in the radial direction and 21 nodes along the vertical. The time step was set equal to 1 year. The integration time was 100 years. Figure 2(a) shows a comparison of radionuclide concentrations along the fracture. Numerical values are plotted versus the approximate analytical results of Reference 8. This shows that there is good agreement between the values. Figure 2(b) shows

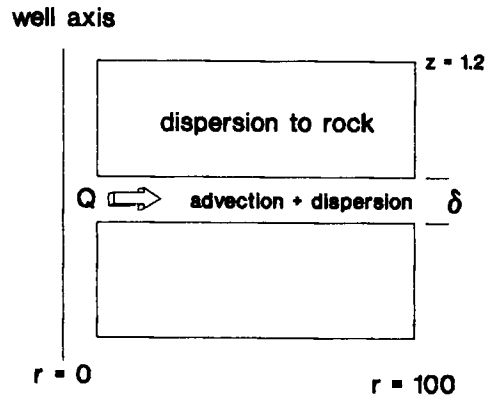

Figure 1. Transport of a radionuclide in a porous rock with a fracture. Problem definition, adapated from Reference 8

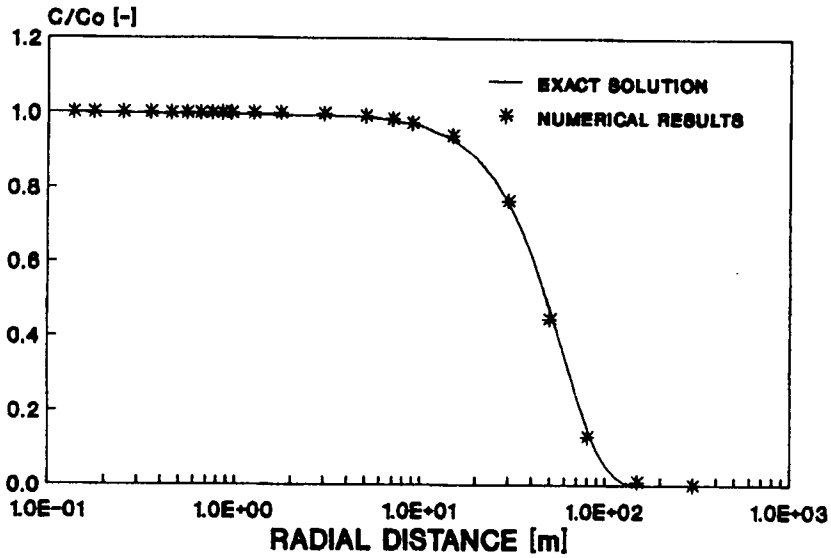

Figure 2(a). Transport of a radionuclide in a porous rock with a fracture. Concentration along the fracture. $K_D = 0\ m^3\ kg^{-1}$, $K_A = 0\ m$

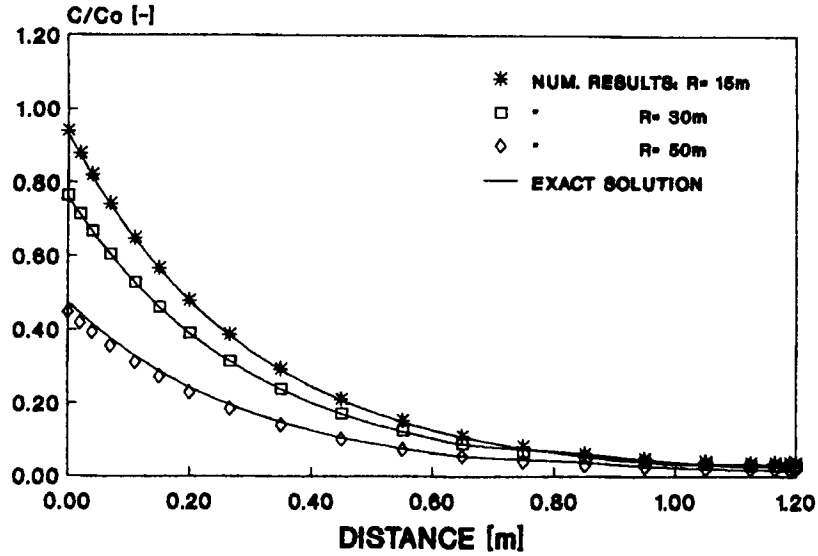

Figure 2(b). Transport of a radionuclide in a porous rock with a fracture. Concentration profiles for $r = 15$, 30 and 50 m. $K_D = 0\ m^3\ kg^{-1}$, $K_A = 0\ m$

concentration profiles for $r = 15$, 30 and 50 m. There is satisfactory adjustment in all these cases. Maximum departures between numerical and analytical results are of the order of 1% for $r = 50$ m.

Case 1(b). The second case considers adsorption both in the rock and in the fracture The analytical solution[8] assumes equilibrium between solute concentrations in the fluid and in the rock. Additionally, equilibrium of solute concentrations in the fluid and in the fracture is also

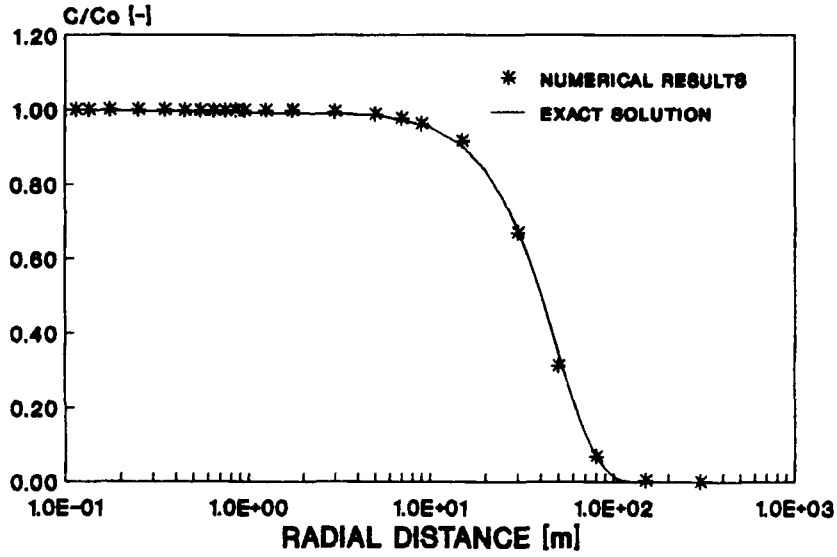

Figure 3. Transport of a radionuclide in a porous rock with a fracture. Concentration along the fracture. $K_D = 3{\cdot}7 \times 10^{-7}$ m^3 kg^{-1}, $K_A = 5 \times 10^{-5}$ m

assumed. In consequence, adsorption is described by the relative values of the constants K_D and K_A. Their ratio induces a delay for retention for solute advection and diffusion. The integration time was again 100 years with 1 year time step.

The variation in solute concentration along the fracture is shown in Figure 3 for $K_D = 3{\cdot}7 \times 10^{-7}$ m^3 kg^{-1} and $K_A = 5 \times 10^{-5}$ m. It compares fairly well with the analytical solution.

Figure 4 shows the comparison between the numerical and the analytical solution for solute

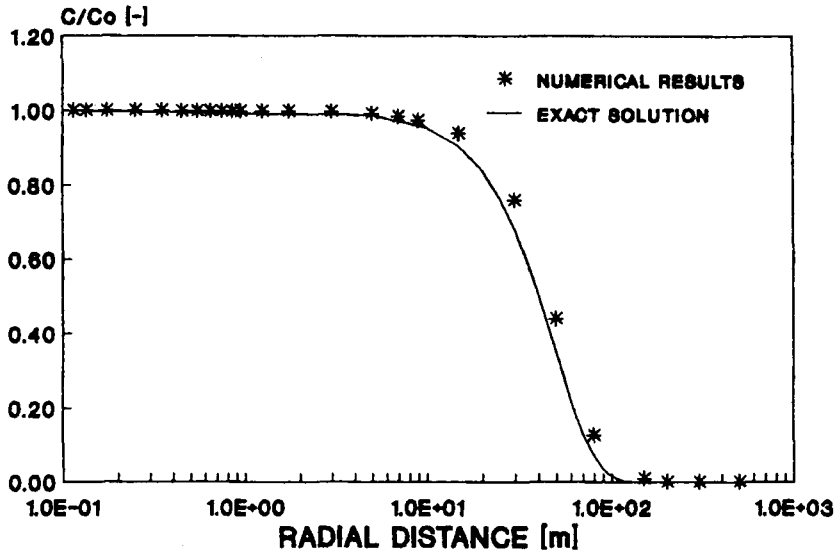

Figure 4. Transport of a radionuclide in a porous rock with a fracture. Concentration along the fracture. $K_D = 0$ m^3 kg^{-1}, $K_A = 5 \times 10^{-5}$ m

concentration along the fracture in the case $K_D = 0\,m^3\,kg^{-1}$ and $K_A = 5 \times 10^{-5}$ m. The adjustment is again satisfactory except for the numerically computed front position. It leads the analytical one by 10–20 m. This represents an error of the order fo 2%.

Case 2

This case consists of comparing the results obtained using the model discussed herein with the experiments reported in Reference 13. These experiments, in the frame of the INTRACOIN project, have been performed in a granitic rock at Finnsjön, thus providing an important source of data. They involve two tracers, one amenable to sorption and the other not sorbed by the rock. The fracture is nearly horizontal.

Figure 5 shows a sketch of the experiment, adapated from Reference 13. Tracers (I^- and Sr^{2+}) were injected at well #2 at constant rate and 100 m depth. Water was pumped from well #1 at constant rate. It was assumed that the water flow converged symmetrically towards well #1 along a plane horizontal fracture of constant aperture. In consequence, advection, diffusion and sorption are considered along the fracture. The time scale for the experiments (600 h) imposes considering a sorption process as described by equation (5).

Water in the porous rock matrix was considered stagnant. Thus tracers are only diffused and sorbed in the equivalent porous rock. It was also assumed that equilibrium conditions prevailed for sorption in the porous rock, as described by equation (3), through a constant transfer coefficient K_D.

The values adopted for the parameters[13] are given in Table I.*

Several rock parameters were measured in the laboratory and are listed in Table II.

Boundary conditions are similar to the ones of case 1, with the exception of those at well #1, where the boundary condition implemented implies conservation of solute mass.[13] Thus

$$\pi r_1^2 h \frac{\partial C}{\partial t} + (Q_P - Q_F)C - 2\pi\delta D_L \frac{\partial C}{\partial r} = 0. \tag{8}$$

Reference 13 gives an analytical solution for this scenario, depending on various parameters (for the rock and the fracture). These parameters were adjusted to reproduce the experimental results.

The adjustment procedure was as follows.

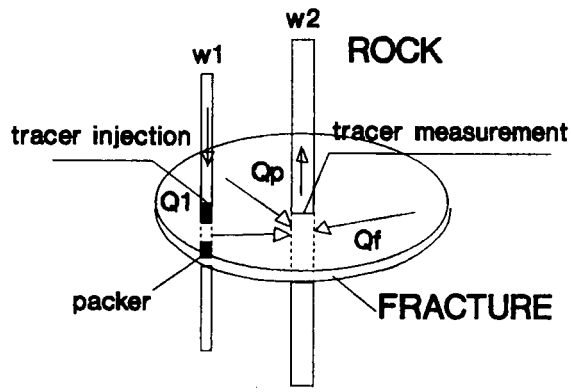

Figure 5. Sketch of the experiment at Finnsjön, adapted from Reference 13.

Table I. Parameter values for Case 2

Parameter	Symbol	Value
Pumping well radius (#1)	r_1	0·11 m
Injection well radius (#2)	r_2	0·11 m
Distance between wells	L	30·0 m
Pumping flow rate	Q_P	$1·0 \times 10^{-4}$ m^3 s^{-1}
Flow rate in fracture	Q_F	$2·0 \times 10^{-5}$ m^3 s^{-1}
Pumping well depth	h	100·0 m
Injection time interval	—	350·0 h
Pumping time interval	—	600·0 h
Injection flow rate	Q_I	$2·7 \times 10^{-7}$ m^3 s^{-1}
Concentration, I^-	—	67·0 mol m^{-3}
Concentration, Sr^{2+}	—	94·0 mol m^{-3}

Table II. Rock parameters measured in laboratory

Parameter	Symbol	Val ue
Rock porosity	ϕ	0·003
Rock density	ρ_B	2700 kg m^{-3}
Effective diffusivity, I^-	$D_e = \phi D$	$0·1 \times 10^{-12}$ m^2 s^{-1}
Effective diffusivity, Sr^{2+}	$D_e = \phi D$	$2·2 \times 10^{-12}$ m^2 s^{-1}
Adsorption coefficient, I^-	K_D	0 m^3 kg^{-1}
Adsorption coefficient, Sr^{2+}	K_D	$2·7 \times 10^{-3}$ m^3 kg^{-1}
Rock capacity, I^-	$\alpha = \phi + \rho_B K_D$	0·003
Rock capacity, Sr^{2+}	$\alpha = \phi + \rho_B K_D$	7·3

1. Hydrodynamic parameters such as water residence time, fracture aperture and hydrodynamic dispersion were adjusted first using the non-sorbable tracer (I^-). Rock diffusion and adsorption were also adjusted.
2. Diffusivity and adsorption parameters were then adjusted for the sorbable tracer (SR^{2+}).

As mentioned above, these values have also been applied for the numerical simulations. Laboratory measurements were also used whenever necessary. Table III defines the values as

Table III. Scenario parameters for I^- migration

Parameter	Symbol	Value
Effective diffusivity times rock capacity	αD_e	$1·3 \times 10^{-13}$ m^2 s^{-1}
Dispersivity parameter	β	370·0 s
Water residence time	t_w	5900 s
Sorption rate constant*	K_S^F	0 s^{-1}
Release rate constant*	K_R^F	0 s^{-1}

* Not adjusted.

given in Reference 13 for I^-. The values for rock porosity and capacity were taken from laboratory measurements.

From the water residence time (t_w) and the flow rate (Q_F) the fracture aperture is obtained as

$$\delta = \frac{Q_F t_w}{\pi(l^2 - r_1^2)} = 4{\cdot}1 \times 10^{-4}\ \text{m}.$$

Thus rock diffusivity was obtained assuming that the rock capacity as measured in the laboratory and the value of αD_e were valid. Thus

$$D = 1{\cdot}44 \times 10^{-8}\ \text{m}^2\ \text{s}^{-1}.$$

Figure 6 shows a satisfactory comparison of numerical results versus experimental ones. A grid consisting 25 nodes in the radial direction and 21 nodes along z was used. The time step was set to 5 h. At the end of the pumping interval (600 h) the present calculation predict 90% tracer recovery. The experimental result was 98%. The exact solution, tuned with optimum parameters, predicted 95% tracer recovery.

The set of parameters given in Table IV have been adjusted in Reference 13 for the sorbable tracer (Sr^{2+}).

Several options were considered to obtain the values for the rock adsorption and diffusion parameters. The product αD_e was always kept as given in Table IV. This is a constraint imposed by the analytical approximation, considered to be valid for the present situation. The computational grid and time step for the I^- calculations were used for these calculations. These options are discussed in what follows.

Figure 7(a) compares the calculated results with the experiments considering the value for α obtained in the laboratory. This leads to $\alpha = 7{\cdot}30$ and $D = 3{\cdot}2 \times 10^{-11}\ \text{m}^2\ \text{s}^{-2}$. The comparison looks terrible.

Figure 7(b) compares the calculated results with the experiments considering the value of D_e

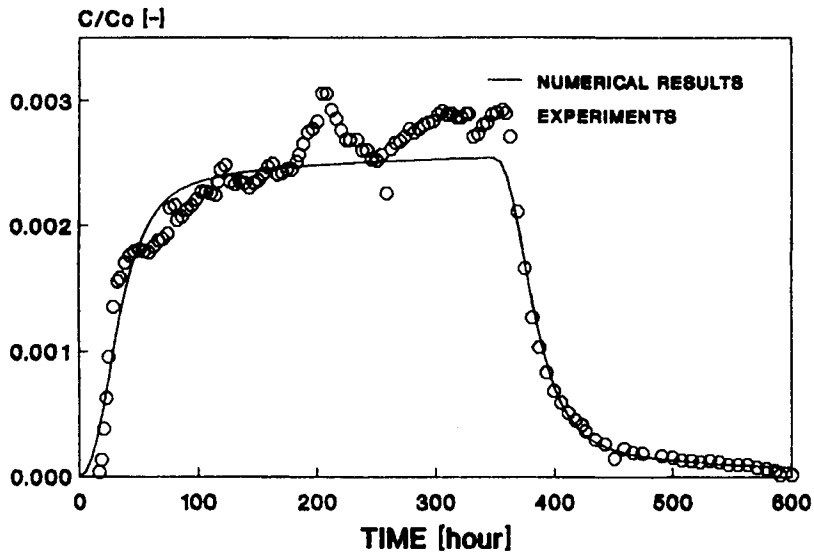

Figure 6. Numerical simulation of the tracer experiment at Finnsjön. Time evolution of I^- concentration. $\alpha = 0{\cdot}003$, $D = 1{\cdot}44 \times 10^{-8}\ \text{m}^2\ \text{s}^{-1}$

Table IV. Scenario parameters for Sr^{2+} migration

Parameter	Symbol	Value
Effective diffusivity times rock capacity	αD_e	$7{\cdot}0 \times 10^{-13}$ m^2 s^{-1}
Dispersivity parameter*	β	370·0 s
Water residence time*	t_w	5900 s
Sorption rate constant	K_S^F	$6{\cdot}3 \times 10^{-6}$ s^{-1}
Release rate constant†	K_R^F	0 s^{-1}

* Same as I^-. † Not adjusted.

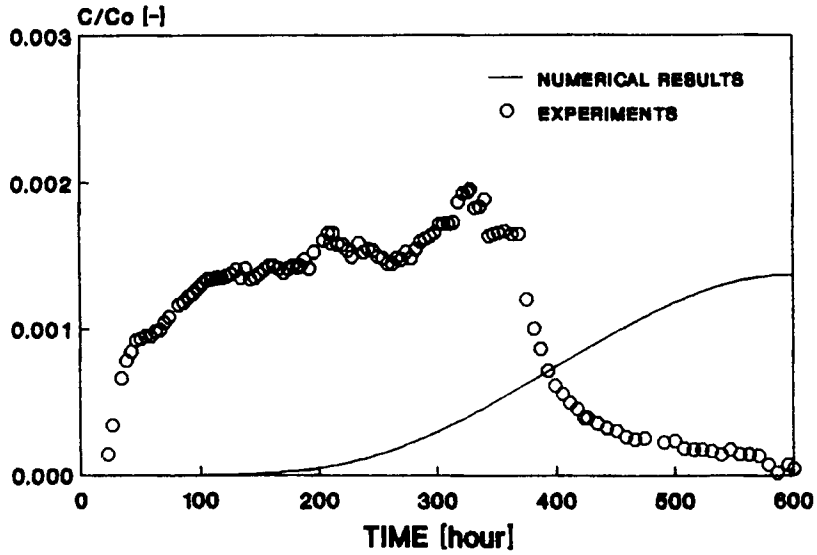

Figure 7(a). Numerical simulation of the tracer experiment at Finnsjön. Time evolution of Sr^{2+} concentration. $\alpha = 7{\cdot}3$, $D = 3{\cdot}2 \times 10^{-11}$ m^2 s^{-1}, $\Delta y = 0{\cdot}005$ m

obtained in the laboratory. This leads to $\alpha = 0{\cdot}32$ and $D = 7{\cdot}3 \times 10^{-11}$ m^2 s^{-1} The comparison is satisfactory.

It is important to recall that αD_e is constant in both cases. The conclusion is that in so far as the analytical solution depends only on this product, then the numerical method fails to describe some transport process. Other cases were tested, leading to the conclusion that cases with strong adsorption were poorly described.

A possible explanation for this behaviour lies in the use of large volumes including a fracture. This in turn implies assigning a false effective volume for the interface phenomena. Should the concentration in the control volume be a close approximation to the fracture concentration, the control volume must have a length scale comparable with the scale of the fracture volume. Thus

fracture volume in cell > porous rock volume times rock capacity.

This leads to

$$\mathscr{V}_f > \alpha(\mathscr{V} - \mathscr{V}_f). \tag{9}$$

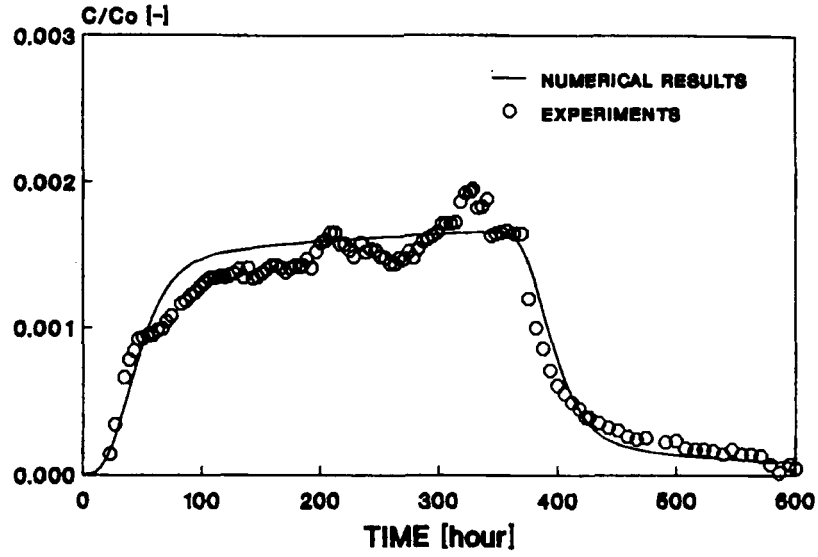

Figure 7(b). Numerical simulation of the tracer experiment at Finnsjön. Time evolution of Sr^{2+} concentration. $\alpha = 0{\cdot}32$, $D = 7{\cdot}3 \times 10^{-11}\ m^2\ s^{-1}$, $\Delta y = 0{\cdot}005$ m

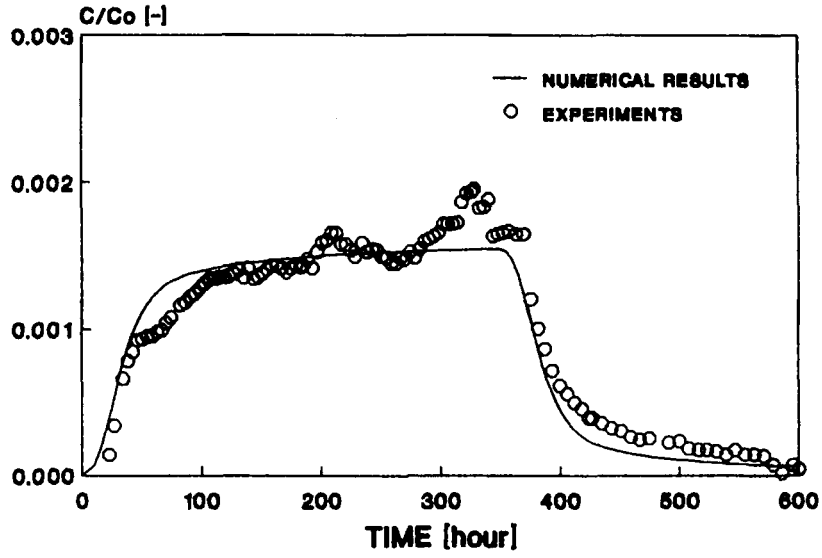

Figure 8. Numerical simulation of the tracer experiment at Finnsjön. Time evolution of Sr^{2+} concentration. $\alpha = 1{\cdot}58$, $D = 4{\cdot}4 \times 10^{-13}\ m^2\ s^{-1}$, $\Delta y = 0{\cdot}0005$ m

For a rectanglar cell of dimensions $\Delta x \times \Delta y$ containing a plane fracture of aperture δ, this in turn implies

$$\Delta x \delta > \alpha(\Delta y - \delta)\Delta x. \tag{10}$$

This condition implies that

$$\Delta y < \delta\left(1 + \frac{1}{\alpha}\right). \tag{11}$$

Several numerical experiments showed that considering condition (11) allowed meaningful results to be obtained

Thus with $\alpha = 1{\cdot}58$ and $D = 4{\cdot}4 \times 10^{-13}$ m^2 s^{-1}, restriction (11) implies $\Delta y < 0{\cdot}001$ m. Using $\Delta y = 0{\cdot}0005$ m, the results shown in Figure 8 are obtained, which compare fairly well with the experiments. Thus it may be concluded that (11) provides a useful criterion to set the discretization.

CONCLUSIONS

An extension of a previous model[6] for the prediction of contaminant dispersion has been presented.

One limitation of the model may be overcome through adequate discretization. The limitation lies in considering a single value for the solute concentration in a control volume including a discrete fracture. A criterion is given to guide the seection of an adequate discretization.

Results obtained complement previous calculations,[5,6] showing high accuracy when compared with analytical results. Results obtained for tracer experiments allowed for a more precise description of sorption phenomena and provided a partial validation of the code.

APPENDIX: NOMENCLATURE

$\mathscr{A}$ area
b volume/wet surface ratio in a fracture
C solute concentration in fluid
D hydrodynamic dispersion coefficient in rock
D_L longitudinal dispersion coefficient in a discrete fracture
F solute concentration per unit mass of rock
K transfer coefficient
l unit vector in plane of a fracture
M diffusion from/to surrounding equivalent porous medium
$\bar{n}$ normal unit vector
q specific discharge
S solute concentration at a surface
u_f fluid velocity in a discrete fracture
$\mathscr{V}$ control volume
$\partial\mathscr{V}$ volume boundary surface
∇ gradient operator

Greek letters

α_L solute dispersion length
β_L dispersivity coefficient
δ fracture thickness (also referred to as fracture aperture)
λ solute radioactive decay constant
ρ density
ϕ porosity

Subscripts and superscripts

B average
ext fracture surface on face of a control volume

F fracture
P porous medium
R recovery or liberation
S sorption

REFERENCES

1. J. C. Ferreri and M. Ventura, 'Numerical aspects of the study of regional thermal impact of radioactive waste repositories', *Nucl. Eng. Design*, **86**, 253–263 (1985).
2. J. C. Ferreri and G. M. Grandi, 'Models for the study of local effects produced by a high-level radioactive waste repository', in C. Taylor, M. D. Olson, P. M. Gresho and W. G. Habashi (eds), *Numerical Methods in Laminar and Turbulent Flows*, Vol. 2, Pineridge, Swansea, 1985, pp. 1257–1267.
3. G. M. Grandi and J. C. Ferreri, 'FRACTURE-BFC: a compuer code for the numerical prediction of hydrodynamics in fractured porous media', in S. Idelsohn (ed.), *Proc. MECOM '85*, October 1985, *Mecánica Computacional*, Vol. 3, AMCA, Santa Fe, 1986, pp. 301–323.
4. G. M. Grandi and J. C. Ferreri, 'Boundary-fitted finite-difference calculations of fluid flow and scalar transport in fractured-porous media', in H. Niki and M. Kawahara (eds), *Proc. Int. Conf. on Computational Methods in Flow Analysis*, Vol. 1, Okayama University of Science, Okayama, 1988, pp. 611–618.
5. G. M. Grandi, 'Modelos computacionales de la hidrodinánica de medios porosos fracturados', *PhD. Thesis*, Instituto Balseiro, Universidad Nacional de Cuyo, 1988; see also CNEA-NT 20/89, CNEA, Buenos Aires, 1989.
6. G. M. Grandi and J. C. Ferreri, 'A computational method for the hydrodynamics of fractured porous media', *Int. j. numer. methods fluids*, **12**, 261–285 (1991).
7. J. Bear, *Dynamics of Fluids in Porous Media*, American Elsevier, New York, 1972.
8. C.-S. Chen, 'Solutions for radionuclide transport from injection well into a single fracture in a porous formation', *Water Resources Res.*, **22**, 508–518 (1986).
9. I. Neretnieks and A. Rasmuson, 'An approach to modelling radionuclide migration in a medium with strongly varying velocity and block sizes along the flow path', *Water Resources Res.*, **20**, 1823–1836 (1984).
10. A. Rasmuson and I. Neretnieks, 'Radionuclide migration in strongly fissured zones: the sensitivity to some assumptions and parameters', *Water Resources Res.*, **22**, 559–569 (1986).
11. A. Rasmuson and I. Neretnieks, 'Migration of radionuclides in fissured rock: the influence of micropore diffusion and longitudinal dispersion', *J. Geophys. Res.*, **86**, 3749–3785 (1981).
12. D. H. Tang *et al.*, 'Comtaminant transport in fractured porous media: analytical solution for a single fracture', *Water resources Res.*, **17**, 555–564 (1981).
13. L. Moreno and I. Neretnieks, 'Evaluation of some tracer test in the granitic rock at Finnsjön', *KBS Tek. Rap. 83-38*, Royal Institute of Technology, Stockholm, 1983.
14. D. Hodgkinson and D. Lever, 'Interpretation of a field experiment on the transport of sorbed and non-sorbed tracers through a fracture in crystalline rock, *Radioact. Waste Manag. Nucl. Fuel Cycle*, **4**, 129–158 (1983).